Linear displacement current solely driven by the quantum metric

Longjun Xiang, [1] Bin Wang, [1,*] Yadong Wei, [1] Zhenhua Qiao, [2] and Jian Wang [1,3,†]
[1] *College of Physics and Optoelectronic Engineering, Shenzhen University, Shenzhen 518060, China*
[2] *Department of Physics, University of Science and Technology of China, Hefei, Anhui 230026, China*
[3] *Department of Physics, The University of Hong Kong, Pokfulam Road, Hong Kong, China*

(Received 23 January 2024; revised 2 February 2024; accepted 23 February 2024; published 12 March 2024)

Quantum metric and Berry curvature are the real part and imaginary part of the quantum geometric tensor, respectively. The $\mathcal{T}$-odd ($\mathcal{T}$, time-reversal) nonlinear Hall effect driven by the quantum metric dipole, recently confirmed in [Science **381**, 181 (2023)] and [Nature (London) **621**, 487 (2023)], established the geometric duality to the $\mathcal{T}$-even nonlinear Hall effect that driven by the Berry curvature dipole. Interestingly, a similar geometric duality between the quantum metric and the Berry curvature, particularly for the *linear response* of Bloch electrons, has not been established, although the $\mathcal{T}$-odd linear intrinsic anomalous Hall effect (IAHE) solely driven by the Berry curvature has been known for a long time. Herein, we develop the quantum theory for displacement current under an AC electric field. Particularly, we show that the $\mathcal{T}$-even component of the linear displacement current conductivity (LDCC) is solely determined by the quantum metric, by both the response theory and the semiclassical theory. Notably, with symmetry analysis we find that the $\mathcal{T}$-even LDCC can contribute a *Hall current* in $\mathcal{T}$-invariant systems but with low symmetry, while its longitudinal component is immune to symmetry. Furthermore, employing the model Hamiltonians, we arrive at a $1/\mu$ (μ, chemical potential) experimental observable enhancement of the displacement current owing to the divergent behavior of quantum metric near Dirac point, similar to the IAHE at Weyl point. Our study reveals the band geometric origin of the linear displacement current and establishes, together with the IAHE, the geometric duality for the *linear response* of Bloch electrons. Additionally, our paper offers the intrinsic Hall effect in $\mathcal{T}$-invariant materials, which cannot be envisioned in DC transport in both linear and nonlinear regimes.

DOI: 10.1103/PhysRevB.109.115121

I. INTRODUCTION

The quantum geometry [1] of Bloch electrons shows a fundamental importance among various fascinating responses of (topological) quantum materials [2–4] under electromagnetic fields, as unveiled by manipulating the symmetry that relates the responses to the band geometric quantities [5–8]. For instance, it has been well understood that the band geometric quantity Berry curvature is responsible for the intrinsic anomalous Hall effect (IAHE) observed in ferromagnetic metals [9], where the time-reversal ($\mathcal{T}$) symmetry is broken owing to the IAHE conductivity tensor solely determined by the $\mathcal{T}$-odd Berry curvature [10], as illustrated in Fig. 1(b). Furthermore, the Berry curvature dipole [13–16] that features the $\mathcal{T}$-even but $\mathcal{P}$-odd ($\mathcal{P}$, space-inversion) properties, can drive the extrinsic nonlinear Hall effect (ENHE) in $\mathcal{T}$-invariant but $\mathcal{P}$-broken systems, as illustrated in Fig. 1(d).

Apart from the well-known Berry curvature, the quantum geometric tensor of Bloch electrons also contains a dual band geometric quantity—the quantum metric [11,17,18], which recently received much attention, but mainly in the form of quantum metric dipole that usually appears in the nonlinear transport of Bloch electrons [12,19–24] and features the $\mathcal{T}$-odd and $\mathcal{P}$-odd properties. Among them, the quantum metric dipole driven intrinsic nonlinear Hall effect (INHE) [12,19,20], as illustrated in Fig. 1(c), has been recently confirmed experimentally in antiferromagnetic topological insulator $MnBi_2Te_4$ [21,22] (that breaks $\mathcal{P}$ and $\mathcal{T}$ symmetries). However, how the quantum metric itself is manifested in the *linear response* of Bloch electrons (as the dual effect of the IAHE) remains elusive, in sharp contrast with the Berry curvature.

On the other hand, we notice that the responses discussed above, as the nonlinear variants of the Ohm's law [25], generally feature the Fermi-surface property [12,13,19,20] and thereby can only be expected in metallic or gapless systems. However, in addition to the conduction current that appears in the metallic solids, the current in Maxwell's equations [26] in fact contains another contribution, namely the displacement current that appears in the insulating solids [27]. Although the connection between the linear/nonlinear responses and the band geometric quantities of the conducting Bloch electrons (electrons on the Fermi surface) has been well established, how the displacement current (even at linear regime) relates to the band geometric quantity is unexplored. In particular, as the cousin of the conduction current, whether or not there exists a Hall effect for the displacement current is also unknown.

In this paper, inspired by the intimate relation between the electric polarization and the displacement current, we develop the quantum theory for the linear displacement current under an AC electric field based on the quantum response theory within independent particle approximation. We show that the linear displacement current conductivity (LDCC) comprises

*bwang@szu.edu.cn
†jianwang@hku.hk

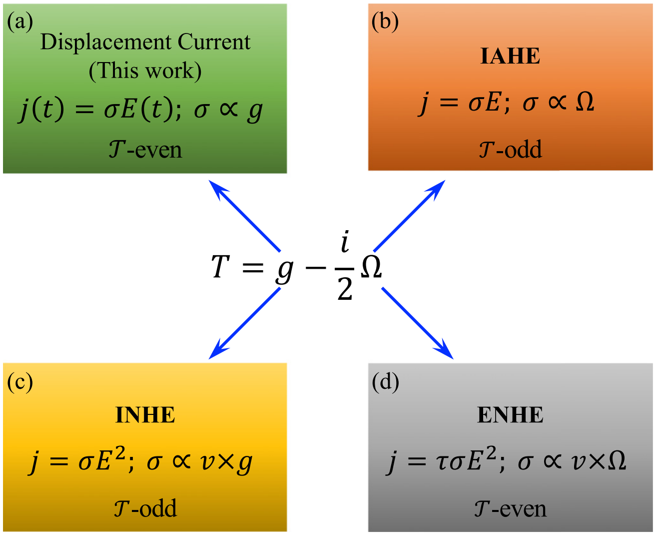

FIG. 1. Guided by symmetry, the quantum geometric tensor $T = g - i\Omega/2$ [11] can be fully probed by four current responses, where g and Ω stand for the quantum metric and the Berry curvature, respectively. (a) The displacement current probes the $\mathcal{T}$-even quantum metric (proposed in this paper). (b) The intrinsic anomalous Hall effect (IAHE) probes the $\mathcal{T}$-odd Berry curvature [9]. (c) The intrinsic nonlinear Hall effect (INHE) probes the $\mathcal{T}$-odd quantum metric dipole $\propto v \times g$ with v the velocity [12]. (d) The extrinsic (proportional to the relaxation time τ) nonlinear Hall effect (ENHE) probes the $\mathcal{T}$-even Berry curvature dipole $\propto v \times \Omega$ [13]. Note that for the second-order nonlinear responses (c) and (d), the $\mathcal{P}$ symmetry of the probed system must be broken, as regulated by the $\mathcal{P}$-odd quantum metric dipole and Berry curvature dipole.

both the $\mathcal{T}$-even and the $\mathcal{T}$-odd contributions. Particularly, we reveal that the $\mathcal{T}$-even DCC is solely determined by the quantum metric. Remarkably, by symmetry analysis, we find that the $\mathcal{T}$-even DCC can allow a transverse component and hence displays a *displacement Hall current* in $\mathcal{T}$-invariant systems but with low symmetry, while its longitudinal component is less restricted by symmetry. As a benchmark, we show that the obtained expressions in adiabatic limit can also be derived by the semiclassical theory accurate up to the second order. Furthermore, using the low-energy model Hamiltonians, we find that the displacement current will be significantly enhanced when the chemical potential is close to the Dirac point where the quantum metric is divergent, similar to the behavior of IAHE at Weyl point. Our study uncovers the band geometric origin of the linear displacement current and establishes, together with the IAHE, the geometric duality for the *linear response* of Bloch electrons, as illustrated in Figs. 1(a) and 1(b). In addition, our paper delivers the very first intrinsic Hall effect in $\mathcal{T}$-invariant systems, which cannot appear in DC transport in both linear and nonlinear regimes, particularly due to the $\mathcal{T}$-odd nature of the intrinsic DC linear and nonlinear conductivities.

II. DISPLACEMENT CURRENT FROM ELECTRIC POLARIZATION

Before presenting the quantum theory, it is instructive to give a heuristic argument on the origin of displacement current. In terms of Maxwell's classical electromagnetic theory, for insulating or gapped systems, the conduction current vanishes due to the lack of free charges. However, an AC electric field $E_\beta(t) = E_\beta \cos(\omega t)$ can generate a displacement current density $J^D_\beta = \partial_t D_\beta$, where $D_\beta \equiv E_\beta(t) + 4\pi\epsilon_0 P_\beta(t)$ is the displacement field with ϵ_0 and P_β the vacuum dielectric constant and the electric polarization induced by the positional shift of bound charges [28], respectively. Interestingly, although the (spontaneous) electric polarization of crystalline solids has been well understood through the geometric phase of Bloch electrons [10], the displacement current seems not to appreciate any geometrical effects and also Hall effect, as far as we know.

Up to the first order of electric field, we find that $P_\beta(t)$ can be expressed as [10,29–34] ($\hbar = e = 1$),

$$P_\beta(t) = -\sum_n \int_k f_n\left[\mathcal{A}^\beta_n + \mathcal{A}^{\beta,E}_n(t)\right], \tag{1}$$

where $\int_k \equiv \int dk^d/(2\pi)^d$ with d the dimension of the system and f_n is the equilibrium Fermi distribution function. In Eq. (1), the intraband Berry connection $\mathcal{A}^\beta_n$ contributes the spontaneous or zero-field electric polarization [29–31,34], while $\mathcal{A}^{\beta,E}_n(t) \equiv G^{\beta\alpha}_n E_\alpha(t)$ is responsible for the field-induced electric polarization linear in the electric field [35–37]. In particular, $G^{\beta\alpha}_n$ is the Berry connection polarizability tensor given by [19,21,22,38,39]

$$G^{\beta\alpha}_n \equiv 2\mathrm{Re}\sum_m \frac{r^\beta_{nm} r^\alpha_{mn}}{\epsilon_n - \epsilon_m}, \tag{2}$$

where $r^\beta_{nm} \equiv \langle u_n | i\partial_\beta | u_m\rangle$ with $m \neq n$ ($|u_n\rangle$: the periodic part of Bloch state) is the interband Berry connection and ϵ_n is the energy for the nth band. We wish to mention that $G^{\beta\alpha}_n$ encodes the information of local quantum metric $g^{\beta\alpha}_{nm} = 2\mathrm{Re}[r^\beta_{nm} r^\alpha_{mn}]$. Particularly, both quantities possess the same symmetry transformation.

By definition, taking the time derivative of field-induced electric polarization, we obtain a linear displacement current with a response equation

$$J^D_\beta = \sigma^D_{\beta\alpha}(t) E_\alpha, \tag{3}$$

where

$$\sigma^D_{\beta\alpha}(t) = \omega \sin(\omega t) \sum_n \int_k f_n G^{\beta\alpha}_n \tag{4}$$

is the LDCC. Note that Eq. (3) together with Eq. (4) displays a formal similarity to the IAHE since they are driven by the real part and the imaginary part of the quantum geometric tensor, respectively, as compared in Figs. 1(a) and 1(b). In fact, they can be derived in a unified way, as will be shown below. Interestingly, we find that $\sigma^D_{\beta\alpha}$ may also include a transverse component σ^D_{yx} when the integral of G^{yx}_n does not vanish. Therefore, a displacement Hall effect in $\mathcal{T}$-invariant systems can be expected due to $\mathcal{T} G^{\beta\alpha}_n = G^{\beta\alpha}_n$.

We wish to remark that the intrinsic linear (charge) Hall effect is forbidden by $\mathcal{T}$ symmetry in the DC case, as dictated by the Onsager relation [9] or the $\mathcal{T}$-odd property of the response coefficient. In general, the linear DC Hall conductivity can be decomposed as

$\sigma_{\alpha\beta} = \sigma^{\rm in}_{\alpha\beta} + \tau\sigma^{\rm ex}_{\alpha\beta}$ [40,41], where the first term is intrinsic but $\mathcal{T}$-odd while the second term is $\mathcal{T}$-even but extrinsic due to the presence of the relaxation time τ [42]. However, for displacement current, we find that the time derivative for the field-induced electric polarization replaces the role of τ in DC case [41] and hence allows the intrinsic $\mathcal{T}$-even linear Hall effect for the displacement current, which cannot show up in DC charge transport.

Up to now, we only present a qualitative discussion. Particularly, Eq. (4) is a hand waving derivation and the rigorous one should be obtained with quantum mechanical calculations, as detailed below. Additionally, we wish to remark that Eq. (4) seems not applicable to gapless systems where the concept of electric polarization is not well defined [40] particularly due to the static electric screening. However, this constraint can be relaxed in AC transport with a high frequency [43].

III. THE QUANTUM THEORY FOR DISPLACEMENT CURRENT

In this section, we formulate the quantum theory for displacement current under an AC electric field based on the quantum response theory [6,44,45]. To be specific, we start from the quantum Liouville equation for the density matrix element ρ_{mn} within independent particle approximation [23,24,44],

$$i\frac{\partial}{\partial t}\rho_{mn} = \epsilon_{mn}\rho_{mn} + i(\rho_{mn})_{;k_\alpha}E_\alpha(t) + \sum_l [r^\alpha_{ml}\rho_{ln}(t) - \rho_{ml}(t)r^\alpha_{ln}]E_\alpha(t), \tag{5}$$

where $(\rho_{mn})_{;k_\alpha} = [\partial_\alpha - i(\mathcal{A}^\alpha_m - \mathcal{A}^\alpha_n)]\rho_{mn}$ with $\partial_\alpha \equiv \partial/\partial k_\alpha$, r^α_{ml} is the interband Berry connection and $E_\alpha(t) = E_\alpha\cos(\omega t) = \frac{1}{2}\sum_{\omega_1} E_\alpha e^{i\omega_1 t}$ with $\omega_1 = \pm\omega$ is the AC electric field. Equation (5) can be recursively solved to obtain a series in increasing powers of the electric field [23,24,44], namely $\rho_{mn} = \sum_{n=1}^\infty \rho^{(n-1)}_{mn}$, where $\rho^{(n-1)}_{mn}$ is proportional to $E^{(n-1)}_\alpha$. To our purpose, with $\rho^{(0)}_{nm} = \delta_{nm}f_n$ [44], the density matrix $\rho^{(1)}_{nm}$ at the first order of electric field can be easily obtained from Eq. (5), which is

$$\rho^{(1)}_{mn} = \frac{1}{2}\sum_{\omega_1}[i\delta_{mn}\partial_\alpha f_m + f_{nm}r^\alpha_{mn}]\frac{E_\alpha e^{-i(\omega_1+i\eta)t}}{\omega_1 - \epsilon_{mn} + i\eta}, \tag{6}$$

where $f_{nm} = f_n - f_m$ and $\eta \to 0^+$ is an infinitesimal quantity. Correspondingly, the current density at the first order of the electric field, defined as $J_\beta \equiv \sum_{mn}\int_k v^\beta_{nm}\rho^{(1)}_{mn}$, is found to be

$$J_\beta = \sum_n\sum_{\omega_1}\int_k v^\beta_n\partial_\alpha f_n E_\alpha\frac{ie^{-i(\omega_1+i\eta)t}}{2(\omega_1+i\eta)} + \sum_{mn}\sum_{\omega_1}\int_k f_{nm}r^\beta_{nm}r^\alpha_{mn}E_\alpha\frac{i\epsilon_{nm}e^{-i(\omega_1+i\eta)t}}{2(\omega_1 - \epsilon_{mn} + i\eta)}, \tag{7}$$

where we have used $v^\beta_{nm} = i\epsilon_{nm}r^\beta_{nm}$ for $n \neq m$. Note that the first term of Eq. (7) is irrelevant to the band geometry of Bloch electrons and corresponds to the familiar extrinsic linear Drude current in DC limit due to $\lim_{\omega_1\to 0} i/(\omega_1 + i\eta) = \tau$ [13]. Besides the extrinsic linear Drude current, we note that Eq. (7) (particularly by the nonresonant contribution of its second term) further contains the well-known intrinsic anomalous Hall current and the overlooked linear displacement current phenomenally discussed above, which is explicitly expressed as

$$J^N_\beta = \sum_{mn}\sum_{\omega_1}\int_k f_{nm}r^\beta_{nm}r^\alpha_{mn}E_\alpha\frac{i\epsilon_{nm}e^{-i\omega_1 t}}{2(\omega_1 - \epsilon_{mn})}. \tag{8}$$

At this stage, by writing $\epsilon_{nm}/(\omega_1 - \epsilon_{mn}) = 1 - \omega_1/(\omega_1 - \epsilon_{mn})$, we find that J_β can be divided into (see Appendix A)

$$J^N_\beta = J^C_\beta + J^D_\beta, \tag{9}$$

where J^C is the intrinsic AC conduction Hall current, given by

$$J^C_\beta = \sum_n\int_k f_n\Omega^{\beta\alpha}_n E_\alpha\cos\omega t, \tag{10}$$

where $\Omega^{\beta\alpha}_n = 2\sum_m {\rm Im}[r^\beta_{nm}r^\alpha_{mn}]$ is the Berry curvature. In DC limit, Eq. (10) is nothing but the intrinsic anomalous Hall current. Furthermore, $J^D_\beta = \partial_t P_\beta$ stands for the intrinsic displacement current, where P_β is the AC polarization defined by

$$P_\beta = \sum_n\int_k f_n[\mathcal{G}^{\beta\alpha}_n\cos\omega t + \mathcal{F}^{\beta\alpha}_n\sin\omega t]E_\alpha. \tag{11}$$

Notably, $\mathcal{G}^{\alpha\beta}_n$ and $\mathcal{F}^{\alpha\beta}_n$ in Eq. (11) encode the information of quantum metric and Berry curvature, respectively, given by

$$\mathcal{G}^{\beta\alpha}_n = \sum_m\frac{\epsilon_{mn}}{\omega^2 - \epsilon^2_{mn}}2{\rm Re}\big[r^\beta_{nm}r^\alpha_{mn}\big], \tag{12}$$

$$\mathcal{F}^{\beta\alpha}_n = \sum_m\frac{\omega}{\omega^2 - \epsilon^2_{mn}}2{\rm Im}\big[r^\beta_{nm}r^\alpha_{mn}\big]. \tag{13}$$

Under $\mathcal{T}$ symmetry, it is easy to show that $\mathcal{T}\mathcal{G}^{\alpha\beta}_n = \mathcal{G}^{\alpha\beta}_n$ while $\mathcal{T}\mathcal{F}^{\alpha\beta}_n = -\mathcal{F}^{\alpha\beta}_n$ due to $\mathcal{T}r^\alpha_{nm} = r^\alpha_{mn}$, and therefore the displacement current in general includes both the $\mathcal{T}$-even and $\mathcal{T}$-odd contributions, similar to the DC shift and injection photocurrent under light illumination [44,46]. Throughout this paper, we focus on the $\mathcal{T}$-invariant systems and hence we will only consider the first term of Eq. (11). Furthermore, under the adiabatic limit, we have $\epsilon_{mn} \gg \omega$ and therefore $\mathcal{G}^{\beta\alpha}_n$ reduces to $G^{\beta\alpha}_n$ given by Eq. (2). As a result, the AC polarization P_β particularly due to the first term of Eq. (11) recovers the field-induced polarization given by the second term of Eq. (1) and the time derivative of P_β further gives the LDCC Eq. (4) phenomenally discussed above.

At this stage, we wish to remark that the LDCC given by Eq. (4) features a Fermi-sea form [23,25,47], which means that the expression for J^D_β can be used for the insulating and also the metallic systems. Furthermore, we emphasize that the intrinsic linear displacement current given by Eq. (3) [or the time derivative of the first term of Eq. (11) particularly under the adiabatic limit] is geometrically dual to Eq. (10), which, respectively, is driven by the Berry curvature and the quantum metric, as compared in Figs. 1(b) and 1(a). Note that the displacement current vanishes in the DC limit ($\omega \to 0$) while Eq. (10) survives in that limit. To close this section, we summarize that Eqs. (11) and (12) [which gives Eqs. (3) and (4) under the adiabatic limit] are the main results in this paper, which can also be derived by the semiclassical theory [10], see Appendix B.

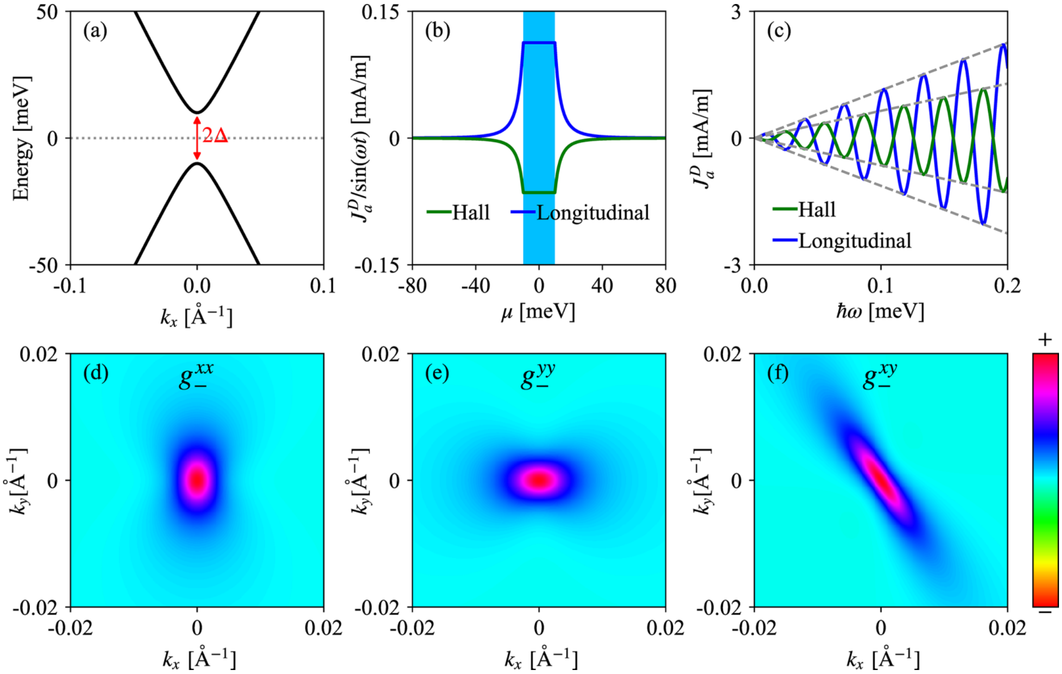

FIG. 2. (a) The band dispersion for Eq. (15) along k_x direction. Here the red-vertical arrow measures the gap and the horizontal-dashed line indicates the chemical potential μ. (b) The μ dependence for the longitudinal and Hall displacement current, given by Eqs. (18) and (20), respectively, by choosing the driving frequency $\omega = 0.01$ meV. Here the vertical shadow highlights the in-gap current plateau. (c) The frequency dependence for the longitudinal and Hall displacement current when μ is placed inside the gap. Here the dashed-grey line indicates the global linear dependence on ω. The $\boldsymbol{k}$-resolved distribution for the quantum metric (d) g_-^{xx}, (e) g_-^{yy}, and (f) g_-^{xy} [here a term $sv_yk_x\sigma_x$ is added to break the mirror symmetries of Eq. (15)].

IV. SYMMETRY CONSTRAINTS

After establishing the quantum theory for the displacement current, we now discuss the symmetry constraints for its conductivity, particularly on its $\mathcal{T}$-even component from 32 crystallographic point groups. Note that the number of independent components of a physical tensor is determined by Neumann's principle [48]. Particularly, for the rank-2 LDCC tensor, we have

$$\sigma^D_{\beta\alpha} = R_{\beta\beta'}R_{\alpha\alpha'}\sigma^D_{\beta'\alpha'}, \tag{14}$$

where $R_{\beta\beta'}$ stands for the matrix element for the point group operation R. Note that Eq. (14) has been implemented by Bilbao Crystallographic Server [49]. As a consequence, by defining the Jahn notation $[V^2]$ [50] for $\sigma^D_{\beta\alpha}$, we find that $\sigma^D_{\beta\beta}$ is allowed by all 32 crystallographic point groups while $\sigma^D_{\beta\alpha}$ with $\alpha \neq \beta$ can only appears in crystallographic point groups with low symmetry: 1, -1, 2, m, $2/m$. Here we wish to remark that the transverse components of $\sigma^D_{\beta\alpha}$ offers the very first intrinsic Hall effect in time-reversal-invariant systems, which cannot appear in DC transport since all the intrinsic DC transport coefficients feature the $\mathcal{T}$-odd nature.

V. MODEL CALCULATIONS

In this section, we illustrate our theory with model Hamiltonians.

A. Two-dimensional massive Dirac model

In this subsection, we employ a two-band massive model to illustrate our general proposal. The low-energy Hamiltonian to describe the massive Dirac fermions located at momenta Λ is given by [13]

$$H_{s\Lambda} = v_xk_x\sigma_y - sv_yk_y\sigma_x + \Delta\sigma_z, \tag{15}$$

where σ_i is the Pauli matrix for pseudospin, $s = \pm 1$, Δ controls the gap magnitude, and $v_{x/y}$ is the Fermi velocity. For simplicity, we ignore the tilt term $s\alpha k_y$ in Ref. [13]. The band dispersion for Eq. (15) is $\epsilon_\pm = \pm h$ with $h = \sqrt{\Delta^2 + v_x^2k_x^2 + v_y^2k_y^2}$, where $+$ $(-)$ denotes the conduction (valence) band, as shown in Fig. 2(a). Note that Eq. (15) possesses the mirror symmetry $\mathcal{M}_y$ due to $\mathcal{M}_ys = -s$, which indicates that the transverse LDCC vanishes by Eq. (14). For the longitudinal LDCC, using Eq. (12) we find

$$\mathcal{G}^{xx}_\pm = \pm\frac{v_x^2\left(v_y^2k_y^2 + \beta^2\right)}{4h^3(h^2 - \omega^2)}, \tag{16}$$

$$\mathcal{G}^{yy}_\pm = \pm\frac{v_y^2\left(v_x^2k_x^2 + \beta^2\right)}{4h^3(h^2 - \omega^2)}. \tag{17}$$

It is easy to see that both $\mathcal{G}^{xx}_\pm$ and $\mathcal{G}^{yy}_\pm$ that are even in k_x and k_y can lead a nonvanishing longitudinal current. We emphasize that $\mathcal{G}^{xx}_\pm$ and $\mathcal{G}^{yy}_\pm$ encode the diagonal contribution of the quantum metric, as displayed in Figs. 2(d) and 2(e), respectively. At zero temperature, the longitudinal displacement current

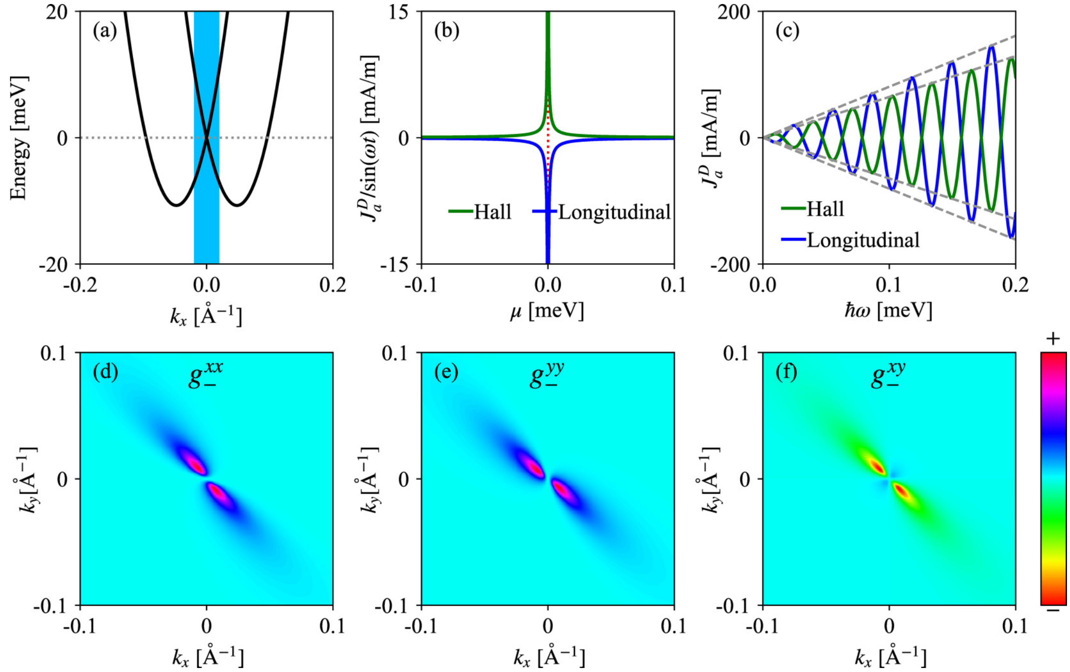

FIG. 3. (a) The band dispersion for Eq. (21) along k_x direction. Here the vertical shadow highlights regime that the displacement current dominates. In addition, the horizontal-dashed line also indicates the chemical potential. (b) The μ dependence for the longitudinal and Hall displacement current, given by Eq. (22), by choosing the driving frequency $\hbar\omega = 10^{-4}$ meV. Here the dashed-red line highlights the divergent behavior at $\mu = 0$. (c) The frequency dependence for the longitudinal and Hall displacement current when $\mu = 0.1$ meV. Here the dashed-grey line indicates the global linear dependence on ω. The $\boldsymbol{k}$-resolved distribution for the quantum metric (d) g_-^{xx}, (e) g_-^{yy}, and (f) g_-^{xy}.

can be directly calculated as (see Appendix C 1)

$$\frac{J_x^D}{E_x} = \frac{J_y^D}{E_y} = \begin{cases} e^2 \dfrac{\Delta^2 7\omega \sin(\omega t)}{48\pi |\mu|^3} & \mu \notin [-\Delta, \Delta], \\ e^2 \dfrac{7\omega \sin(\omega t)}{48\pi \Delta} & \mu \in [-\Delta, \Delta], \end{cases} \tag{18}$$

where μ is the chemical potential. Note that have used $\Delta \gg \hbar\omega$ and $v_x = v_y$ [13]. Here the elementary charge e is restored by dimension analysis. By Eq. (18), we find that the longitudinal displacement current will quickly decrease to zero when the chemical potential μ is away from the gap, whereas a longitudinal LDCC plateau can be obtained when μ is located inside the gap, as shown in Fig. 2(b). Note the the longitudinal displacement current shows a global linear dependence on the driving frequency ω, as shown in Fig. 2(c) and therefore will disappear in DC transport. For the gapped situation, one can easily obtain the AC polarization from the displacement current, $P_x/E_x = P_y/E_y = 7e^2/(48\pi\Delta)\cos(\omega t)$, which shows explicitly that AC polarization will be stronger when the gap decreases.

To acquire a nonzero displacement Hall current, we break the mirror symmetry $\mathcal{M}_y$ of Eq. (15) by introducing an additional term $sv_yk_x\sigma_x$, which may be physically realized by strain effects [51], and then we have

$$G_\pm^{xy} = \mp \frac{v_y^2\left(v_x^2 k_x k_y - \Delta^2\right)}{4\left(v_x^2k_x^2 + v_y^2(k_x+k_y)^2 + \Delta^2\right)^{5/2}}, \tag{19}$$

where we have adopted the adiabatic limit. Equation (19) encodes the off-diagonal information of the quantum metric, as shown in Fig. 2(f). In a similar way, the displacement Hall current at zero temperature is found to be (see Appendix C 2)

$$\frac{J_x^D}{E_y} = \begin{cases} -e^2 \dfrac{\Delta^2 \omega \sin(\omega t)}{12\pi |\mu|^3} & \mu \notin [-\Delta, \Delta], \\ -e^2 \dfrac{\omega \sin(\omega t)}{12\pi \Delta} & \mu \in [-\Delta, \Delta], \end{cases} \tag{20}$$

which shows the same behavior with the longitudinal displacement current, as compared in Figs. 2(b) and 2(c). Note that the magnitude of the linear displacement current is determined by the dimensionless factor $\sim\hbar\omega/\Delta$, which indicates that this effect will be significantly enhanced when the gap $\Delta \to 0$ when the driving frequency ω is fixed, as shown below.

B. Two-dimensional spin-orbit-coupled electron gas

Next we evaluate the displacement current with a gapless model. Particularly, we consider the low-energy effective Hamiltonian for two-dimensional spin-orbit-coupled electron gas with crystallographic point group 2, which is constructed by adding Rashba and Dresselhaus spin-orbit coupling and is written as [52–54]

$$H = E_0 + \lambda_R(k_y\sigma_x - k_x\sigma_y) + \lambda_D(k_x\sigma_x - k_y\sigma_y), \tag{21}$$

where $E_0 = k^2/2m$ with $k^2 = k_x^2 + k_y^2$. The band dispersions for Eq. (21) are given by $\epsilon_\pm = E_0 \pm \sqrt{(\lambda_D k_y + \lambda_R k_x)^2 + (\lambda_D k_x + \lambda_R k_y)^2}$ with $\pm$ the valance band and conduction band, respectively, as shown in Fig. 3(a). Focusing on the band crossing regime [as highlighted by the vertical shadow in Fig. 3(a)], which in fact corresponds to the massless Dirac Hamiltonian, the linear displacement current under adiabatic limit at zero temperature can be evaluated (see Appendix C 3),

$$J_a^D = \frac{e^2}{\hbar}\frac{\hbar\omega}{|\mu|}C_{ab}E_b \sin(\omega t) \quad a, b \in \{x, y\}, \tag{22}$$

where $C_{xy} = -\lambda_R\lambda_D/[8\pi(\lambda_R^2 - \lambda_D^2)]$ and $C_{xx} = C_{yy} = (\lambda_R^2 + \lambda_D^2)/[16\pi(\lambda_R^2 - \lambda_D^2)]$. Note that Eq. (22) shows a $|\mu|^{-1}$ dependence and does not show a conductivity plateau due to the lack of a finite gap, as shown Fig. 3(b). Due to this divergent behavior, an enhanced displacement current can be achieved with a relatively low driving frequency compared to the gapped situation, as shown in Fig. 3(c). In addition, in Figs. 3(d)–3(f), the corresponding $\boldsymbol{k}$-resolved distribution for the diagonal and off-diagonal components of the quantum metric are shown, which are responsible for the divergent behavior of the linear displacement current, in a similar way to the divergent IAHE in the point-node Weyl point.

VI. SUMMARY

In summary, we formulate the quantum theory for displacement current under an AC electric field. We show that the $\mathcal{T}$-even LDCC is solely determined by the quantum metric. In terms of symmetry analysis, we find that the longitudinal component of the LDCC is immune to symmetry meanwhile its Hall component can be expected even in $\mathcal{T}$-invariant systems but with low symmetry, such as the strained transition metal dichalcogenides (TMDCs) monolayers, the strained surface of topological crystalline insulators, and the insulating two-dimensional chiral twisting graphene or TMDCs [55–59]. Furthermore, our model calculations demonstrate that an enhanced displacement current can be achieved in the massless Dirac point, such as in two-dimensional graphene monolayer, where the quantum metric shows a divergent behavior like the Berry curvature in the Weyl point.

To the experiment aspect, we note that a (0.1–10) GHz AC electric field may be applied to generate an observable displacement current signal based on our model calculations. We wish to mention that such a high-frequency AC electric field [60] has been used to generate the nonlinear Hall signal driven by the Berry curvature dipole. Furthermore, the lock-in technique operated at GHz regime [7] may be employed to detect the generated longitudinal and transverse AC currents. In addition, the linear dependence on chemical potential μ particularly near gap closing point highlights the gate tunability in experiments [61].

Last but not least, our paper reveals the band geometric origin of the linear displacement current and in turn, offers a desirable tool to detect the quantum metric of Bloch electrons in quantum materials. Importantly, our paper together with the IAHE establishes the geometric duality for the *linear response* of Bloch electrons. In addition, the transverse displacement current also provides the very first Hall effect in $\mathcal{T}$-invariant materials, which is forbidden by $\mathcal{T}$ symmetry in DC transport. Beyond these, the linear displacement current in point-node Weyl semimetals (which also appreciates the $1/\mu$ divergent behavior) may be employed to realize the low-energy high-speed photodetection particularly in terahertz regime [62–64], which will be explored in the future.

ACKNOWLEDGMENT

J.W. thanks the financial support from the National Natural Science Foundation of China (Grant No. 12034014).

APPENDIX A: THE DETAILED DERIVATIONS FOR EQS. (10)–(13)

In this Appendix, we show the detailed derivation for Eqs. (10)–(13) given in the main text. Particularly, by writing

$$\frac{\epsilon_{nm}}{\omega_1 - \epsilon_{mn}} = 1 - \frac{\omega_1}{\omega_1 - \epsilon_{mn}}, \tag{A1}$$

we find that J_β^N given by Eq. (8) in the main text can be divided into

$$J_\beta^N = J_\beta^C + J_\beta^D, \tag{A2}$$

where

$$\begin{aligned} J_\beta^C &\equiv \frac{1}{2}\sum_{nm}\sum_{\omega_1=\pm\omega}\int_k f_{nm}r_{nm}^\beta r_{mn}^\alpha E_\alpha i e^{-i\omega_1 t} \\ &= \sum_{nm}\int_k f_{nm}r_{nm}^\beta r_{mn}^\alpha E_\alpha i\cos(\omega t) \\ &= \sum_n\int_k f_n\Omega_n^{\beta\alpha}E_\alpha\cos\omega t, \end{aligned} \tag{A3}$$

as given by Eq. (10) in the main text. Here the last term is obtained by interchanging the dummy index and $\Omega_n^{\beta\alpha} = i\sum_m(r_{nm}^\beta r_{mn}^\alpha - r_{nm}^\alpha r_{mn}^\beta)$ is the Berry curvature. Furthermore, for the remaining term of J_β^N, we have

$$J_\beta^D = \sum_{nm}\sum_{\omega_1} f_{nm}r_{nm}^\beta r_{mn}^\alpha E_\alpha\frac{-i\omega_1 e^{-i\omega_1 t}}{2(\omega_1 - \epsilon_{mn})} = \partial_t P_\beta(t), \tag{A4}$$

where

$$\begin{aligned} P_\beta &\equiv \sum_{nm}\sum_{\omega_1} f_{nm}r_{nm}^\beta r_{mn}^\alpha E_\alpha\frac{e^{-i\omega_1 t}}{2(\omega_1 - \epsilon_{mn})} \\ &= \sum_{nm} f_{nm}r_{nm}^\beta r_{mn}^\alpha E_\alpha\left[\frac{e^{i\omega t}}{2(-\omega - \epsilon_{mn})} + \frac{e^{-i\omega t}}{2(\omega - \epsilon_{mn})}\right] \\ &= \sum_{nm} f_{nm}r_{nm}^\beta r_{mn}^\alpha E_\alpha\frac{\epsilon_{mn}\cos(\omega t) - i\omega\sin(\omega t)}{\omega^2 - \epsilon_{mn}^2} \\ &= \sum_n\int_k f_n[\mathcal{G}_n^{\beta\alpha}\cos\omega t + \mathcal{F}_n^{\beta\alpha}\sin\omega t]E_\alpha, \end{aligned} \tag{A5}$$

as given by Eq. (11) in the main text. Note that the last term of Eq. (A5) is also obtained by interchanging dummy index and $\mathcal{G}_n^{\alpha\beta}$ and $\mathcal{F}_n^{\alpha\beta}$, respectively, is defined as

$$\mathcal{G}_n^{\beta\alpha} = \sum_m\frac{\epsilon_{mn}}{\omega^2 - \epsilon_{mn}^2}2\mathrm{Re}[r_{nm}^\beta r_{mn}^\alpha], \tag{A6}$$

$$\mathcal{F}_n^{\beta\alpha} = \sum_m\frac{\omega}{\omega^2 - \epsilon_{mn}^2}2\mathrm{Im}[r_{nm}^\beta r_{mn}^\alpha], \tag{A7}$$

as given by Eqs. (12) and (13) in the main text.

APPENDIX B: THE SEMICLASSICAL FORMULATION FOR DISPLACEMENT CURRENT

In this Appendix, we show that the displacement current can also be derived with the semiclassical theory accurate up to the second order of the electric field. In particular, under a time-dependent but slowly perturbed electric field, the semiclassical equation of motions for Bloch electrons up to the second order of electric field are given by [10,19,34,65,66]

$$\dot{\boldsymbol{r}} = \bar{\boldsymbol{v}}_{\boldsymbol{k}} - \dot{\boldsymbol{k}} \times \bar{\boldsymbol{\Omega}} - \bar{\boldsymbol{\Omega}}_{\boldsymbol{k}t}, \quad \dot{\boldsymbol{k}} = -\boldsymbol{E}(t), \tag{B1}$$

where $\bar{\boldsymbol{v}}_{\boldsymbol{k}} = \nabla_{\boldsymbol{k}}\bar{\epsilon}_k$ is the band velocity that considers the field-induced correction, $\bar{\boldsymbol{\Omega}} = \nabla_{\boldsymbol{k}} \times \bar{\boldsymbol{\mathcal{A}}}$ is the Berry curvature that also considers the field-induced correction, and $\bar{\Omega}^{\alpha}_{\boldsymbol{k}t} = \partial_\alpha \mathcal{A}^t - \partial_t \bar{\mathcal{A}}^\alpha$ is the Berry curvature defined in the $(\boldsymbol{k}, t)$ parameter space, where $\mathcal{A}^t = \langle \bar{u}|i\partial_t|\bar{u}\rangle$ with $|\bar{u}\rangle$ the time-dependent Bloch state, and $\bar{\mathcal{A}}^\alpha = \mathcal{A}^\alpha + \mathcal{A}^{\alpha,E}$ stands for the Berry connection up to the first order of electric field. By solving Eq. (B1), we find

$$\dot{\boldsymbol{r}} = \bar{\boldsymbol{v}}_{\boldsymbol{k}} + \boldsymbol{E}(t) \times \bar{\boldsymbol{\Omega}} - \bar{\boldsymbol{\Omega}}_{\boldsymbol{k}t}. \tag{B2}$$

Correspondingly, the intrinsic current density, defined as $\boldsymbol{J} = \int_k f\dot{\boldsymbol{r}}$, is given by

$$\boldsymbol{J} = \int_k f[\bar{\boldsymbol{v}}_{\boldsymbol{k}} + \boldsymbol{E}(t) \times \bar{\boldsymbol{\Omega}} - \bar{\boldsymbol{\Omega}}_{\boldsymbol{k}t}]. \tag{B3}$$

Furthermore, by restoring the band summation and focusing on the linear intrinsic current response, from the last two terms of Eq. (B3) we obtain

$$J_\beta = \sum_n \int_k f_n[\Omega^{\beta\alpha}_n E_\alpha(t) + G^{\beta\alpha}_n \partial_t E_\alpha(t)], \tag{B4}$$

which corresponds to the conduction current induced by Berry curvature and the displacement current induced by quantum metric, respectively, as given by Eq. (10) and the adiabatic contribution of Eq. (12) [that is Eq. (4)] in quantum theory, respectively. Note that the first term $\bar{\boldsymbol{v}}$ of Eq. (B3) cannot contribute a linear current due to $\bar{\epsilon}_n = \epsilon - 1/2E_\alpha(t)G^{\alpha\beta}_n E_\beta$ [40]. In addition, for the last term of Eq. (B3), we have used $\mathcal{A}^{\alpha,E}_n = G^{\beta\alpha}_n E_\alpha(t)$ for $\partial_t \bar{\mathcal{A}}^\alpha_n$ and ignored $\partial_\alpha \mathcal{A}^t_n$ since $\mathcal{A}^t_n \equiv \langle \bar{u}_n|i\partial_t|\bar{u}_n\rangle$ with $|\bar{u}_n\rangle = |u_n\rangle + \sum_{m\neq n}(\boldsymbol{E}\cdot\boldsymbol{r}_{mn}/\epsilon_{mn})|u_m\rangle$ cannot lead a contribution linear in the electric field. Finally, we wish to remark that the semiclassical formulation is also valid for gapless systems since the concept of electric polarization is not used in the derivation. In fact, the static screening for metal in AC transport is not well defined [43].

APPENDIX C: THE CALCULATION DETAILS FOR EQS. (18), (20), AND (22)

In this Appendix, we present the calculation details for Eqs. (18), (20), and (22), given in the main text.

1. Eq. (18)

For Dirac Hamiltonian Eq. (15), the frequency-dependent integrand for the nonvanishing displacement current conductivity is reproduced as

$$\mathcal{G}^{xx}_\pm = \pm\frac{v_x^2(v_y^2k_y^2 + \Delta^2)}{h^3(4h^2 - \omega^2)}, \quad \mathcal{G}^{yy}_\pm = \pm\frac{v_y^2(v_x^2k_x^2 + \Delta^2)}{h^3(4h^2 - \omega^2)}, \tag{C1}$$

where $h^2 = v_x^2k_x^2 + v_y^2k_y^2 + \beta^2$. When the chemical potential $\mu \in [-\Delta, \Delta]$, at zero temperature we find that

$$\begin{aligned} J^D_x &= -E_x\omega\sin(\omega t)\int_k \mathcal{G}^{xx}_- = -E_x\omega\sin(\omega t)\iint\frac{dk_xdk_y}{4\pi^2}\frac{v_x^2(v_y^2k_y^2 + \Delta^2)}{(v_x^2k_x^2 + v_y^2k_y^2 + \Delta^2)^{3/2}[\omega^2 - 4(v_x^2k_x^2 + v_y^2k_y^2 + \Delta^2)]} \\ &= -\frac{E_x\omega\sin(\omega t)v_x}{4\pi^2v_y}\iint d\bar{k}_xd\bar{k}_y\frac{\bar{k}_y^2 + \Delta^2}{(\bar{k}_x^2 + \bar{k}_y^2 + \Delta^2)^{3/2}[\omega^2 - 4(\bar{k}_x^2 + \bar{k}_y^2 + \Delta^2)]} \end{aligned} \tag{C2}$$

where we have set $\bar{k}_x = v_xk_x$ and $\bar{k}_y = v_yk_y$. Let $(\bar{k}_x, \bar{k}_y) = \bar{k}(\cos\theta, \sin\theta)$, we find

$$\begin{aligned} J^D_x &= -\frac{E_x\omega\sin(\omega t)v_x}{4\pi^2v_y}\int_0^{+\infty}\int_0^{2\pi}\bar{k}d\bar{k}d\theta\frac{\bar{k}^2\sin^2\theta + \Delta^2}{(\bar{k}^2 + \Delta^2)^{3/2}[\omega^2 - 4(\bar{k}^2 + \Delta^2)]} \\ &= -\frac{E_x\omega\sin(\omega t)v_x}{4\pi v_y}\int_0^{+\infty}\bar{k}d\bar{k}\frac{\bar{k}^2 + 2\Delta^2}{(\bar{k}^2 + \Delta^2)^{3/2}[\omega^2 - 4(\bar{k}^2 + \Delta^2)]} \end{aligned} \tag{C3}$$

Furthermore, let $u^2 = \bar{k}^2 + \Delta^2$, we have $\bar{k}d\bar{k} = udu$ and find

$$
\begin{aligned}
J_x^D &= -\frac{E_x\omega\sin(\omega t)v_x}{4\pi v_y}\int_{\Delta}^{+\infty}\frac{u^2+\Delta^2}{u^3(\omega^2-4u^2)}udu = -\frac{E_x\omega\sin(\omega t)v_x}{4\pi v_y}\left(\int_{\Delta}^{+\infty}\frac{1}{\omega^2-4u^2}du + \Delta^2\int_{\Delta}^{+\infty}\frac{1}{u^2(\omega^2-4u^2)}du\right)\\
&= -\frac{\Delta^2 E_x\omega\sin(\omega t)v_x}{4\pi v_y}\int_{\Delta}^{+\infty}\left[\frac{1}{2\omega\Delta^2}\left(\frac{1}{\omega-2u}+\frac{1}{\omega+2u}\right)+\frac{1}{\omega^2u^2}+\frac{2}{\omega^3}\left(\frac{1}{\omega+2u}+\frac{1}{\omega-2u}\right)\right]du\\
&= -\frac{\Delta^2 E_x\sin(\omega t)v_x}{4\pi v_y}\left[\frac{1}{2\Delta^2}\left(\frac{1}{2}\ln\left|\frac{2u+\omega}{2u-\omega}\right|\right)_{\Delta}^{+\infty}+\frac{1}{\omega}\left(-\frac{1}{u}\right)_{\Delta}^{+\infty}+\frac{2}{\omega^2}\left(\frac{1}{2}\ln\left|\frac{2u+\omega}{2u-\omega}\right|\right)_{\Delta}^{+\infty}\right]\\
&= -\frac{\Delta^2 E_x\sin(\omega t)v_x}{4\pi v_y}\left[\frac{1}{\omega\Delta}-\left(\frac{1}{4\Delta^2}+\frac{1}{\omega^2}\right)\ln\left|\frac{2\Delta+\omega}{2\Delta-\omega}\right|\right], \qquad \text{(C4)}
\end{aligned}
$$

Following a similar way, we have

$$
J_y^D = -\frac{\Delta^2 E_y\sin(\omega t)v_y}{4\pi v_x}\left[\frac{1}{\omega\Delta}-\left(\frac{1}{4\Delta^2}+\frac{1}{\omega^2}\right)\ln\left|\frac{2\Delta+\omega}{2\Delta-\omega}\right|\right]. \qquad \text{(C5)}
$$

In addition, when the chemical potential μ penetrates the lower band, we find

$$
J_x^D = -\frac{E_x\omega\sin(\omega t)v_x}{4\pi v_y}\int_{\sqrt{\mu^2-\Delta^2}}^{+\infty}\frac{\bar{k}^2+2\Delta^2}{(\bar{k}^2+\Delta^2)^{3/2}[\omega^2-4(\bar{k}^2+\Delta^2)]}\bar{k}d\bar{k}, \qquad \text{(C6)}
$$

$$
J_y^D = -\frac{E_y\omega\sin(\omega t)v_y}{4\pi v_x}\int_{\sqrt{\mu^2-\Delta^2}}^{+\infty}\frac{\bar{k}^2+2\Delta^2}{(\bar{k}^2+\Delta^2)^{3/2}[\omega^2-4(\bar{k}^2+\Delta^2)]}\bar{k}d\bar{k}, \qquad \text{(C7)}
$$

which can be similarly calculated as

$$
J_x^D = -\frac{\Delta^2 E_x\sin(\omega t)v_x}{4\pi v_y}\left[\frac{1}{\omega|\mu|}-\left(\frac{1}{4|\mu|^2}+\frac{1}{\omega^2}\right)\ln\left|\frac{2|\mu|+\omega}{2|\mu|-\omega}\right|\right], \qquad \text{(C8)}
$$

$$
J_y^D = -\frac{\Delta^2 E_y\sin(\omega t)v_y}{4\pi v_x}\left[\frac{1}{\omega|\mu|}-\left(\frac{1}{4|\mu|^2}+\frac{1}{\omega^2}\right)\ln\left|\frac{2|\mu|+\omega}{2|\mu|-\omega}\right|\right]. \qquad \text{(C9)}
$$

This is true when the Fermi level penetrates the upper band, where we need to sum over the bands. By assuming that $\Delta \gg \hbar\omega$, we find

$$
\ln\left|\frac{1+\omega/2|\Delta|}{1-\omega/2|\Delta|}\right| = \omega/|\Delta| + \omega^3/3|\Delta|^3 + O(\omega^5/|\Delta|^5), \qquad \text{(C10)}
$$

$$
\ln\left|\frac{1+\omega/2|\mu|}{1-\omega/2|\mu|}\right| = \omega/|\mu| + \omega^3/3|\mu|^3 + O(\omega^5/|\mu|^5), \qquad \text{(C11)}
$$

therefore we finally obtain

$$
J_x^D = \begin{cases} \dfrac{e^2}{\hbar}\dfrac{7\hbar\omega E_x\sin(\omega t)v_x}{48\pi\Delta v_y}, & \mu\in[-\Delta,\Delta] \\ \dfrac{e^2}{\hbar}\dfrac{7\hbar\omega\Delta^2 E_x\sin(\omega t)v_x}{48\pi|\mu|^3 v_y}, & \mu\notin[-\Delta,\Delta] \end{cases}, \quad J_y^D = \begin{cases} \dfrac{e^2}{\hbar}\dfrac{7\hbar\omega E_y\sin(\omega t)v_y}{48\pi\Delta v_x}, & \mu\in[-\Delta,\Delta] \\ \dfrac{e^2}{\hbar}\dfrac{7\hbar\omega\Delta^2 E_y\sin(\omega t)v_y}{48\pi|\mu|^3 v_x}, & \mu\notin[-\Delta,\Delta] \end{cases} \qquad \text{(C12)}
$$

which gives the Eq. (18) by taking $v_x = v_y$ in the main text, where e and $\hbar$ are restored by dimension analysis.

2. Eq. (20)

By introducing an additional term $sv_yk_x\sigma_x$ into Eq. (15) (that breaks mirror symmetry $\mathcal{M}_y$), the off-diagonal integrand under the adiabatic limit is given by

$$
G_{\pm}^{xy} = \mp\frac{v_y^2\left(v_x^2k_xk_y-\Delta^2\right)}{4\left(v_x^2k_x^2+v_y^2(k_x+k_y)^2+\Delta^2\right)^{5/2}} = \mp\frac{v_x^2\left(v_x^2k^2\sin\theta\cos\theta-\Delta^2\right)}{4\left[v_x^2k^2(\cos^2\theta+1+2\sin\theta\cos\theta)+\Delta^2\right]^{5/2}}, \qquad \text{(C13)}
$$

where we have assumed $v_x = v_y$ and used the polar coordinate, $\boldsymbol{k} = k(\cos\theta, \sin\theta)$. When the chemical potential μ is inside the gap, we find

$$\sigma_{xy}^{D} \equiv \frac{J_x}{\omega E_y \sin\omega t} = \frac{1}{4\pi^2}\int_0^\infty\int_0^{2\pi} \frac{v_x^2\left(v_x^2k^2\sin\theta\cos\theta - \Delta^2\right)}{4\left[v_x^2k^2(\cos^2\theta + 1 + 2\sin\theta\cos\theta) + \Delta^2\right]^{5/2}} k dk d\theta$$
$$= \frac{1}{8\pi^2}\int_0^\infty\int_0^{2\pi} \frac{v_x^2\left(v_x^2k^2\sin\theta\cos\theta - \Delta^2\right)}{4\left[v_x^2k^2(\cos^2\theta + 1 + 2\sin\theta\cos\theta) + \Delta^2\right]^{5/2}} dk^2 d\theta. \tag{C14}$$

Let $u = v_x^2k^2(\cos^2\theta + 1 + 2\sin\theta\cos\theta) + \Delta^2$, we find

$$k^2 = \frac{u - \Delta^2}{v_x^2(\cos^2\theta + 1 + 2\sin\theta\cos\theta)}, \quad dk^2 = \frac{du}{v_x^2(\cos^2\theta + 1 + 2\sin\theta\cos\theta)}. \tag{C15}$$

Therefore, we have

$$\sigma_{xy}^{D} = \frac{1}{32\pi^2}\left(\int_{\Delta^2}^\infty\int_0^{2\pi} \frac{v_x^4\sin\theta\cos\theta(u-\Delta^2)}{v_x^4(\cos^2\theta + 1 + 2\sin\theta\cos\theta)^2u^{5/2}} du d\theta - \int_{\Delta^2}^\infty\int_0^{2\pi} \frac{v_x^2\Delta^2}{v_x^2(\cos^2\theta + 1 + 2\sin\theta\cos\theta)u^{5/2}} du d\theta\right)$$
$$= -\frac{1}{12\pi\Delta} \tag{C16}$$

where we have used

$$\int_{\Delta^2}^\infty \frac{1}{u^{5/2}} du = \frac{2}{3\Delta^3}, \quad \int_{\Delta^2}^\infty \frac{1}{u^{3/2}} du = \frac{2}{\Delta}, \tag{C17}$$

and

$$\int_0^{2\pi} \frac{\sin\theta\cos\theta}{(\cos^2\theta + 1 + 2\sin\theta\cos\theta)^2} d\theta = -\pi, \quad \int_0^{2\pi} \frac{1}{(\cos^2\theta + 1 + 2\sin\theta\cos\theta)} d\theta = 2\pi. \tag{C18}$$

In a similar way, when the chemical potential μ penetrates the bands, we find

$$\sigma_{xy}^{D} = -\frac{\Delta^2}{12|\mu|^3}. \tag{C19}$$

Equation (C16) together with Eq. (C19) gives the Eq. (20) in the main text.

3. Eq. (22)

Within the adiabatic limit, $\mathcal{G}_\pm^{ab}$ reduces to the Berry connection polarizability tensor $G_\pm^{ab}$, which for Eq. (21) are given by

$$G_\pm^{xx} = \pm\frac{\left(\lambda_D^2 - \lambda_R^2\right)^2k_y^2}{4\left[(\lambda_Dk_y + \lambda_Rk_x)^2 + (\lambda_Dk_x + \lambda_Rk_y)^2\right]^{5/2}}, \tag{C20}$$

$$G_\pm^{yy} = \pm\frac{\left(\lambda_D^2 - \lambda_R^2\right)^2k_x^2}{4\left[(\lambda_Dk_y + \lambda_Rk_x)^2 + (\lambda_Dk_x + \lambda_Rk_y)^2\right]^{5/2}}, \tag{C21}$$

$$G_\pm^{yx} = \mp\frac{\left(\lambda_D^2 - \lambda_R^2\right)^2k_xk_y}{4\left[(\lambda_Dk_y + \lambda_Rk_x)^2 + (\lambda_Dk_x + \lambda_Rk_y)^2\right]^{5/2}}. \tag{C22}$$

We first focus on the Hall component. Particularly, when the chemical potential μ penetrates the lower band, at zero temperature we find

$$J_y^D = \omega E_x \sin(\omega t)\int_k \Theta(\mu - \epsilon_-)G_-^{xy} = \frac{\omega E_x\sin(\omega t)}{(2\pi)^2}\iint \frac{\Theta(\mu-\epsilon_-)\left(\lambda_D^2 - \lambda_R^2\right)^2k_xk_y}{4\left[(\lambda_Dk_y + \lambda_Rk_x)^2 + (\lambda_Dk_x + \lambda_Rk_y)^2\right]^{5/2}} dk_x dk_y. \tag{C23}$$

Let

$$x = \lambda_Dk_y + \lambda_Rk_x, \quad y = \lambda_Dk_x + \lambda_Rk_y, \tag{C24}$$

we find

$$k_x = \frac{\lambda_Rx - \lambda_Dy}{\lambda_R^2 - \lambda_D^2}, \quad k_y = \frac{\lambda_Dx - \lambda_Ry}{\lambda_D^2 - \lambda_R^2}.$$

Therefore

$$\left(\lambda_R^2-\lambda_D^2\right)^2k_x^2=\lambda_R^2x^2+\lambda_D^2y^2-2\lambda_R\lambda_Dxy,\quad \left(\lambda_R^2-\lambda_D^2\right)^2k_y^2=\lambda_D^2x^2+\lambda_R^2y^2-2\lambda_R\lambda_Dxy, \tag{C25}$$

$$\left(\lambda_R^2-\lambda_D^2\right)^2k_xk_y=\left(\lambda_R^2+\lambda_D^2\right)xy-\lambda_R\lambda_D(x^2+y^2),\quad \epsilon_\pm=\pm\sqrt{x^2+y^2}. \tag{C26}$$

where we have dropped the E_0 term in $\epsilon_\pm$ by focusing on the linear dispersion regime. Correspondingly, the Jacobi determinant is given by

$$J=\left|\frac{\partial(k_x,k_y)}{\partial(x,y)}\right|=\begin{pmatrix}+\dfrac{\lambda_R}{\lambda_R^2-\lambda_D^2} & -\dfrac{\lambda_D}{\lambda_R^2-\lambda_D^2}\\ +\dfrac{\lambda_D}{\lambda_D^2-\lambda_R^2} & -\dfrac{\lambda_R}{\lambda_D^2-\lambda_R^2}\end{pmatrix}=\frac{\lambda_R^2-\lambda_D^2}{\left(\lambda_R^2-\lambda_D^2\right)^2}=\frac{1}{\lambda_R^2-\lambda_D^2}. \tag{C27}$$

Substituting Eqs. (C24)–(C27) into Eq. (C23) we obtain

$$\begin{aligned}J_y^D&=-\frac{\lambda_R\lambda_D\omega E_x\sin(\omega t)}{16\pi^2\left(\lambda_R^2-\lambda_D^2\right)}\iint\Theta(\mu+\sqrt{x^2+y^2})\frac{1}{(x^2+y^2)^{3/2}}dxdy=-\frac{\lambda_R\lambda_D\omega E_x\sin(\omega t)}{16\pi^2\left(\lambda_R^2-\lambda_D^2\right)}\int_0^\infty\int_0^{2\pi}\Theta(\mu+\rho)\frac{1}{\rho^3}\rho d\rho d\theta\\&=-\frac{\lambda_R\lambda_D\omega E_x\sin(\omega t)}{8\pi\left(\lambda_R^2-\lambda_D^2\right)}\int_{-\mu}^\infty\frac{1}{\rho^2}d\rho=-\frac{e^2}{\hbar}\frac{\hbar\omega}{|\mu|}C_{yx}E_x\sin(\omega t),\end{aligned} \tag{C28}$$

as given by Eq. (22) in the main text, where $C_{yx}=\lambda_R\lambda_D/[8\pi(\lambda_R^2-\lambda_D^2)]$ and we have restored the e and $\hbar$ by dimension analysis. Note that we obtain the same result when the chemical potential μ penetrates the upper band, which can be derived as follows:

$$J_y^D=-\frac{\lambda_R\lambda_D\omega E_x\sin(\omega t)}{8\pi\left(\lambda_R^2-\lambda_D^2\right)}\int_0^\infty\frac{1}{\rho^2}d\rho+\frac{\lambda_R\lambda_D\omega E_x\sin(\omega t)}{8\pi\left(\lambda_R^2-\lambda_D^2\right)}\int_0^\mu\frac{1}{\rho^2}d\rho=-\frac{e^2}{\hbar}\frac{\hbar\omega}{|\mu|}C_{yx}E_x\sin(\omega t). \tag{C29}$$

In a similar way, the longitudinal linear displacement current can be evaluated as

$$J_a^D=\frac{e^2}{\hbar}\frac{\hbar\omega}{|\mu|}C_{aa}E_a\sin(\omega t), \tag{C30}$$

as also given by Eq. (22) in the main text, where $C_{aa}=(\lambda_R^2+\lambda_D^2)/[16\pi(\lambda_R^2-\lambda_D^2)]$.

[1] P. Törmä, Phys. Rev. Lett. **131**, 240001 (2023).
[2] Y. Tokura, M. Kawasaki, and N. Nagaosa, Nat. Phys. **13**, 1056 (2017).
[3] B. Keimer and J. E. Moore, Nat. Phys. **13**, 1045 (2017).
[4] J. W. Xiao and B. H. Yan, Nat. Rev. Phys. **3**, 283 (2021).
[5] J. Y. Ahn, G. Y. Guo, N. Nagaosa, and A. Vishwanath, Nat. Phys. **18**, 290 (2022).
[6] Q. Ma, R. K. Kumar, S.-Y. Xu, F. H. L. Koppens, and J. C. W. Song, Nat. Rev. Phys. **5**, 170 (2023).
[7] Q. Ma, A. G. Grushin, and K. S. Burch, Nat. Mater. **20**, 1601 (2021).
[8] Y. Tokura and N. Nagaosa, Nat. Commun. **9**, 3740 (2018).
[9] N. Nagaosa, J. Sinova, S. Onoda, A. H. MacDonald, and N. P. Ong, Rev. Mod. Phys. **82**, 1539 (2010)
[10] D. Xiao, M.-C. Chang, and Q. Niu, Rev. Mod. Phys. **82**, 1959 (2010).
[11] G. P. Provost and G. Vallee, Commut. Math. Phys. **76**, 289 (1980).
[12] C. Wang, Y. Gao, and D. Xiao, Phys. Rev. Lett. **127**, 277201 (2021).
[13] I. Sodemann and L. Fu, Phys. Rev. Lett. **115**, 216806 (2015).
[14] Q. Ma, S.-Y. Xu, H. Shen, D. MacNeill, V. Fatemi, T.-R. Chang, A. M. M. Valdivia, S. Wu, Z. Du, C.-H. Hsu *et al.*, Nature (London) **565**, 337 (2019).
[15] K. Kang, T. Li, E. Sohn, J. Shan, and K. F. Mak, Nat. Mater. **18**, 324 (2019).
[16] Z. Z. Du, H.-Z. Lu, and X. C. Xie, Nat. Rev. Phys. **3**, 744 (2021).
[17] J. Anandan and Y. Aharonov, Phys. Rev. Lett. **65**, 1697 (1990).
[18] M. V. Berry, Proc. R. Soc. London A **392**, 45 (1984).
[19] Y. Gao, S. A. Yang, and Q. Niu, Phys. Rev. Lett. **112**, 166601 (2014).
[20] H. Y. Liu, J. Z. Zhao, Y.-X. Huang, W. K. Wu, X.-L. Sheng, C. Xiao, and S. A. Yang, Phys. Rev. Lett. **127**, 277202 (2021).
[21] A. Gao *et al.*, Science **381**, 181 (2023).
[22] N. Wang, D. Kaplan, Z. Zhang, T. Holder, N. Cao, A. Wang, X. Zhou, F. Zhou, Z. Jiang, C. Zhang *et al.*, Nature (London) **621**, 487 (2023).
[23] K. Das, S. Lahiri, R. B. Atencia, D. Culcer, and A. Agarwal, Phys. Rev. B **108**, L201405 (2023).
[24] Y. D. Wang, Z. F. Zhang, Z.-G. Zhu, and G. Su, Phys. Rev. B **109**, 085419 (2024).
[25] S. Murakami, N. Nagaosa, and S.-C. Zhang, Science **301**, 1348 (2003).
[26] J. D. Jackson, *Classical Electrodynamics* (John Wiley, Hobeken, NJ, 1998).
[27] M. P. Marder, *Condensed Matter Physics* (John Wiley & Sons, Hoboken, NJ, 2010).
[28] N. Nagaosa, Ann. Phys. **447**, 169146 (2022).

[29] R. D. King-Smith and D. Vanderbilt, Phys. Rev. B **47**, 1651 (1993).
[30] D. Vanderbilt and R. D. King-Smith, Phys. Rev. B **48**, 4442 (1993).
[31] R. Resta, Rev. Mod. Phys. **66**, 899 (1994).
[32] I. Souza, T. Wilkens, and R. M. Martin, Phys. Rev. B **62**, 1666 (2000).
[33] G. Ortiz and A. A. Aligia, Phys. Status Solidi B **220**, 737 (2000).
[34] C. Xiao, B. Xiong, and Q. Niu, Phys. Rev. B **104**, 064433 (2021).
[35] C. Aversa and J. E. Sipe, Phys. Rev. B **52**, 14636 (1995).
[36] R. W. Nunes and X. Gonze, Phys. Rev. B **63**, 155107 (2001).
[37] I. Souza, J. Iniguez, and D. Vanderbilt, Phys. Rev. Lett. **89**, 117602 (2002).
[38] C. Wang, R.-C. Xiao, H. Y. Liu, Z. Zhang, S. Lai, C. Zhu, H. Cai, N. Wang, S. Chen, Y. Deng *et al.*, Natl. Sci. Rev. **9**, nwac020 (2022).
[39] S. Lai, H. Liu, Z. Zhang, J. Zhao, X. Feng, N. Wang, C. Tang, Y. Liu, K. S. Novoselov, S. A. Yang, and W.-B. Gao, Nat. Nanotechnol. **16**, 869 (2021).
[40] C. Xiao, W. Wu, H. Wang, Y.-X. Huang, X. Feng, H. Liu, G.-Y. Guo, Q. Niu, and S. A. Yang, Phys. Rev. Lett. **130**, 166302 (2023).
[41] C. Chen, D. Zhai, C. Xiao, and W. Yao, arXiv:2303.09973.
[42] D. Zhai, C. Chen, C. Xiao, and W. Yao, Nat. Commun. **14**, 1961 (2023).
[43] K. Arakawa, T. Hayashida, K. Kimura, R. Misawa, T. Nagai, T. Miyamoto, H. Okamoto, F. Iga, and T. Kimura, Phys. Rev. Lett. **131**, 236702 (2023).
[44] J. E. Sipe and A. I. Shkrebtii, Phys. Rev. B **61**, 5337 (2000).
[45] J. E. Moore and J. Orenstein, Phys. Rev. Lett. **105**, 026805 (2010).
[46] H. Wang and X. F. Qian, npj Comput. Mater. **6**, 199 (2020).
[47] Here the Fermi-sea form of LDCC means that this conductivity is determined by all states below the Fermi level.
[48] R. E. Newnham, *Properties of Materials: Anisotropy, Symmetry, Structure* (Oxford University Press, Oxford, 2005).
[49] S. V. Gallego, J. Etxebarria, L. Elcoro, E. S. Tasci, and J. M. Perez-Mato, Acta Crystallogr. Sect. A **75**, 438 (2019).
[50] C.-P. Zhang, X.-J. Gao, Y.-M. Xie, H. C. Po, and K. T. Law, Phys. Rev. B **107**, 115142 (2023).
[51] B. T. Zhou, C. P. Zhang, and K. T. Law, Phys. Rev. Appl. **13**, 024053 (2020).
[52] J. Schliemann and D. Loss, Phys. Rev. B **68**, 165311 (2003).
[53] S. Q. Shen, Phys. Rev. B **70**, 081311(R) (2004).
[54] O. Pal and T. K. Ghosh, Phys. Rev. B **109**, 035202 (2024).
[55] E. Y. Andrei and A. H. MacDonald, Nat. Mater. **19**, 1265 (2020).
[56] L. Balents, C. R. Dean, D. K. Efetov, and A. F. Young, Nat. Phys. **16**, 725 (2020).
[57] D. M. Kennes, M. Claassen, L. D. Xian, A. Georges, A. J. Millis, J. Hone, C. R. Dean, D. N. Basov, A. N. Pasupathy, and A. Rubio, Nat. Phys. **17**, 155 (2021).
[58] E. Y. Andrei, D. K. Efetov, P. Jarillo-Herrero, A. H. MacDonald, K. F. Mak, T. Senthil, E. Tutuc, A. Yazdani, and A. F. Young, Nat. Rev. Mater. **6**, 201 (2021).
[59] C. N. Lau, M. W. Bockrath, K. F. Mak, and F. Zhang, Nature (London) **602**, 41 (2022).
[60] D. Kumar, C.-H. Hsu, R. Sharma, T.-R. Chang, P. Yu, J. Y. Wang, G. Eda, G. Liang, and H. Yang, Nat. Nanotechnol. **16**, 421 (2021).
[61] T.-Y. Zhao, A.-Q. Wang, X.-G. Ye, X.-Y. Liu, X. Liao, and Z.-M. Liao, Phys. Rev. Lett. **131**, 186302 (2023).
[62] J. Ahn, G. Y. Guo, and N. Nagaosa, Phys. Rev. X **10**, 041041 (2020).
[63] J. Liu, F. Xia, D. Xiao, F. J. G. de Abajo, and D. Sun, Nat. Mater. **19**, 830 (2020).
[64] Y. Zhang and L. Fu, Proc. Natl. Acad. Sci. USA **118**, e2100736118 (2021).
[65] O. Bleu, G. Malpuech, Y. Gao, and D. D. Solnyshkov, Phys. Rev. Lett. **121**, 020401 (2018).
[66] Z. Liu, Z. H. Qiao, Y. Gao, and Q. Niu, Phys. Rev. Res. **6**, L012005 (2024).